Original Article
ISSN (Online): 2582-7472

ShodhKosh: Journal of Visual and Performing Arts
June 2024 5(6), 1488–1498

RMSE POWER COEFFICIENT OF WIND TURBINES WITH INVERSE TOQUE-SPEED CONTROL

Rishikesh Choudhary[1], Kumar Jyotiraditya[2], Dipo Mahto[3]

[1]Assistant Professor, Department of Electrical Engineering, Bhagalpur College of Engineering, Bhagalpur, India
[2]Assistant Professor, Department of Mechanical Engineering, Bhagalpur College of Engineering, Bhagalpur, India
[3]Professor and Head, Department of Physics, Bhagalpur College of Engineering, Bhagalpur, India

DOI
10.29121/shodhkosh.v5.i6.2024.2409

Funding: This research received no specific grant from any funding agency in the public, commercial, or not-for-profit sectors.

ABSTRACT

The Blade Element Momentum (BEM) method stands out among various turbine modelling techniques due to its integration of airfoil aerodynamics with momentum theory, allowing detailed force calculations on blade elements. While traditional methods like BEM and Wake Models are efficient for initial turbine design, advancements in computational power have enabled the use of Computational Fluid Dynamics (CFD) for more accurate simulations. Although these models are precise, they are computationally intensive, leading to the continued use of simpler empirical methods, such as the static power coefficient approach, in power system studies. Future research aims to validate and implement dynamic estimation models to account for wind variability and turbine control dynamics. Traditional constant torque-speed control strategies maintain a constant generator speed by using a fixed electromagnetic torque command and adjusting the pitch angle when wind speed exceeds the rated value. However, if the pitch control does not respond quickly enough, rotor acceleration can occur, leading to increased power beyond the generator's rating. To mitigate this, the pitch control mechanism must react promptly to adjust the turbine's torque profile, ensuring convergence to the rated operating point and avoiding prolonged generator overload. To reduce the burden on the pitch-control system, an inverse torque-speed control approach is proposed, where the electromagnetic torque is dynamically adjusted based on real-time rotor speed data. This method aims to achieve rated power operation with improved responsiveness and reduced stress on the pitch-control mechanism.

Keywords: RMSE Power Coefficient, Static Power Coefficient, BEM, Constant Power Scheme, Inverse Power Scheme

1. INTRODUCTION

In recent decades, wind energy conversion systems have garnered significant attention due to the depletion of conventional energy resources, increasing demands in industrializing countries, and environmental concerns stemming from emissions. The global energy crisis has been extensively analysed [1], resulting in various proposed solutions. A comprehensive bibliographic review [2] highlights future directions in wind energy research. Researchers worldwide are focused on optimizing wind energy systems, which produce zero carbon emissions and have minimal fuel costs, making them a sustainable alternative for meeting energy needs.

The aerodynamic subsystem dictates the interaction between the wind stream field and the turbine blades. The motion of a high-speed body within a fluid can generate aero-acoustic noise; thus, the tip speed must be maintained within acceptable limits [3]. The aerodynamics resulting from the wind flow over the airfoil design of the turbine blades creates a complex interplay of dynamic lift and drag forces acting on various sections of the blades [4]. This intricate distribution of forces, particularly the lift forces, generates rotational moments that produce useful rotational torque in a specific direction, while the undesirable components contribute to structural stresses and fatigue. By employing modern design

techniques, turbine designers aim to achieve an optimal design that minimizes unwanted structural stresses while maximizing the turbine's energy extraction capacity [5]. Consequently, understanding and appreciating the airflow dynamics in its entirety is essential for accurately modeling this subsystem. Inaccurate modeling can lead to suboptimal designs, resulting in decreased energy yield and increased structural loads, ultimately leading to higher capital and maintenance costs. Generally, electrical engineers may overlook this complex aerodynamic interaction, delegating the modeling challenge to turbine designers. In essence, electrical engineers often confine their focus to the final mechanical torque exerted on the turbine blade (treating it as a lumped inertia) without considering the intricacies of the torque production mechanism arising from the complex dynamics of the turbine-wind interaction [6].

The 1-D momentum method, Swirl Momentum Theory, Blade Element Momentum Method (BEM), Computational Fluid Dynamics (CFD), and wake methods represent a selection of analytical and numerical techniques employed by turbine designers to model aerodynamic subsystems in detail. Among these, the BEM method is particularly advantageous as it incorporates blade design, specifically airfoil aerodynamics, alongside momentum theory, which is not considered in traditional momentum approaches. In the BEM method, the blades are segmented into small airfoil elemental sections, each approximated by a planar model, allowing for the derivation of expressions for the forces acting on the various blade elements. The lift and drag coefficients (C_L and C_D) are the two fundamental parameters derived from this method. Forces acting on different sections of the blade are calculated as a function of the angle of attack, and the local forces are integrated along the blade's longitudinal axis to determine the overall values [7].

The aforementioned methods have been widely utilized in the initial stages of design; however, significant advancements in computational capabilities have enabled the adoption of more detailed Computational Fluid Dynamics (CFD) methods. In CFD approaches, a numerically approximated model of the Navier-Stokes equations is employed to characterize fluid flow [8] [9] [10]. Wake methods take into account the rotational momentum transferred to the wind fluid by the turbine's rotation, both upstream and downstream. Given the complexity of this subsystem, these methods are computationally intensive and require substantial memory for simulations [11]. Nonetheless, various methodologies related to wind speed refinement models have been proposed to incorporate aerodynamic effects into power system studies [12] [13].

The analytical and computational methods discussed above are widely applied in turbine design and energy yield evaluation, as these applications necessitate detailed modeling. However, in power system studies, such intricate modeling is often omitted for the sake of simplicity, leading to the use of generic empirical methods. Among these, static power coefficient methods and dynamic power coefficient methods are the most commonly employed empirical approaches. In these power coefficient methods, the expression for the power extracted by the wind turbine is represented in Equation (1).

$$P_{WT} = P_W . C_P \qquad (1)$$

In the Blade Element Momentum (BEM) method, the power coefficient is determined by integrating the torque contributions from different sections along the longitudinal axis of the blade, resulting in a computationally intensive process. Consequently, numerical approximations are often recommended to express the power coefficient, as shown in Equation (2a), in terms of two independent variables: the tip-speed ratio and the pitch angle. Equation (3) provides the expression for extracted power primarily in terms of wind speed, turbine speed, and rotor size. However, this expression is static in nature, as it assumes that wind speed and turbine speed are at steady-state constant values. In reality, these variables may exhibit dynamic changes due to wind speed variability and control adjustments, potentially leading to dynamic stall and dynamic inflow.

Currently, only the static power coefficient method has been utilized. Future research may explore the implementation of dynamic models following comprehensive validation of the dynamic stall and dynamic wake phenomena.

2. STATIC POWER COEFFICIENT METHOD

Rather than providing explicit mathematical expressions for the power coefficient (C_P), turbine manufacturers typically present this information in complex functional forms or as look-up tables. However, an explicit mathematical expression is essential in an academic context for estimating the power extracted across a specified operating range.

Various equations and estimators, including state observers, have been developed to represent C_P. Among these, several estimators utilize polynomial approaches [14], neural networks, and Newton-Raphson based nonlinear methods [15]. Additionally, several generic equations have been employed to fit the power coefficient curve, including exponential models, sinusoidal models, and polynomial models [15].

The widely adopted generic exponential model is expressed in terms of the tip-speed ratio and the blade pitch angle.

$$C_P(\lambda,\beta) = c_1\left(\frac{c_2}{\lambda_i} - c_3\beta - c_4\beta^{C_5} - c_6\right).\exp\left(-\frac{c_7}{\lambda_i}\right) + c_8\lambda + c_{11} \qquad (2a)$$

$$\text{Where } \lambda_i = \left(\frac{1}{\lambda + c_9\beta}\right) - \left(\frac{c_{10}}{\beta^3 + 1}\right) \qquad (2b)$$

Tip-speed ratio is the ratio of tip speed of the blade to the wind speed and is expressed by $\lambda = \frac{\omega_T R}{v}$ (2c)

Here ω_T is the rotational speed of the turbine in rad/sec, R is radius of the turbine and v is the wind speed in meter/sec.

$$P_{WT} = P_W.C_P(\lambda,\beta) = \frac{1}{2}\rho.\pi R^2.v^3.C_P(\lambda,\beta) \qquad (3)$$

The above static algebraic model has been found to be approximating varied ranges of turbine design and wind conditions by properly estimating the c_i coefficients (Table 1).

Data Set	c_1	c_2	c_3	c_4	c_5	c_6	c_7	c_8	c_9	c_{10}	c_{11}
I	0.5176	116	0.40	0	0	5	21	0.0068	0.08	0.035	0
II	0.44	125	0	0	0	6.94	16.5	0	0	-0.002	0
III	0.22	116	0.40	0	0	5	12.5	0	0.08	0.035	0
IV	0.73	151	0.58	0.002	2.14	13.2	18.4	0	-0.02	-0.003	0

Table1: Typical Power Coefficient for different WTs.

The power coefficient curves for different typical design parameters give in Table 1 have been drawn in Figure 1.

3. ESTIMATION TECHNIQUE FOR POWER COEFFICIENT

Several estimation techniques can be employed to encapsulate the power coefficient into an explicit mathematical expression [15]. Among these, the multivariable polynomial model and the sinusoidal model have been developed as follows:

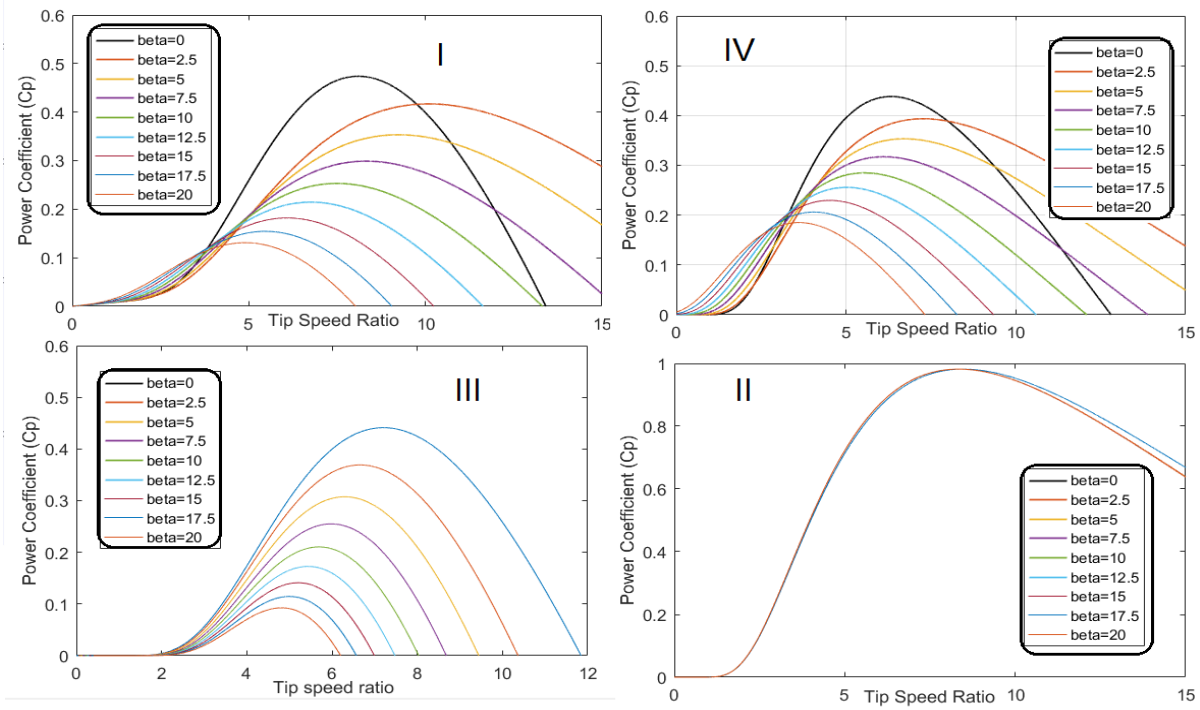

Figure 1: Power coefficient curves for different typical design

3.1 TWO VARIABLE POLYNOMIAL MODELS

The expression for R^{th} order multivariate polynomial estimation model

$$\hat{C}_P(\lambda,\beta)=\sum_{j,k}\zeta_{jk}\lambda^j\beta^k \qquad (4)$$

The above summation is over all $i \in W$, $j \in W$ which satisfies the following condition $\{i \le R \,\&\, j \le R \,\&\, i+j \le R\}$. Here W is the set of whole number. Each term of the above summation shall have a coefficient ζ_{jk} . The total number of unique terms in the above estimator expression shall be equal to the total number of coefficients.

Total number of terms=Total number of coefficients =N= $\frac{R^2+3R+2}{2}$. (5)

$$C_P(\lambda,\beta)=\hat{C}_P(\lambda,\beta)+\varepsilon \qquad (6)$$

$$C_P(\lambda,\beta)=\sum_{j,k}\zeta_{jk}\lambda^j\beta^k+\varepsilon \qquad (7)$$

For total number of M measurements the above equation can be sorted into the matrix equations

$$[C_P]_{M\times 1}=[A]_{M\times N}[\zeta]_{N\times 1`}+[\varepsilon]_{M\times 1} \qquad (8)$$

Parametric Table of Multivariable Estimation of Different Orders				
Parameters	**IInd order**	**IIIrd order**	**IVth order**	**Vth order**
ξ_{00}	0.2413	0.2402	0.2385	0.2387
ξ_{10}	-0.03469	0.04018	0.04111	0.004395
ξ_{01}	-0.1214	-0.1366	-0.1343	-0.07151
ξ_{20}	-0.1307	-0.1302	-0.2069	-0.2068
ξ_{11}	-0.1116	-0.1109	-0.2072	-0.2068
ξ_{02}	-0.02687	-0.02587	0.02927	0.02861
ξ_{30}	NA	-0.02549	-0.02545	-0.002819
ξ_{21}	NA	-0.01373	-0.01471	-0.04287
ξ_{12}	NA	-0.02974	-0.03075	0.03807
ξ_{03}	NA	0.01571	0.01466	-0.04868
ξ_{40}	NA	NA	0.03743	0.03727
ξ_{31}	NA	NA	0.02744	0.02734
ξ_{22}	NA	NA	-0.0177	-0.01739
ξ_{13}	NA	NA	0.02668	0.02643
ξ_{04}	NA	NA	-0.01433	-0.01413
ξ_{50}	NA	NA	NA	-0.005928
ξ_{41}	NA	NA	NA	-0.004832
ξ_{32}	NA	NA	NA	-0.003309
ξ_{23}	NA	NA	NA	0.02248
ξ_{14}	NA	NA	NA	-0.0246
ξ_{50}	NA	NA	NA	0.01238
RMSE	**0.06566**	**0.05461**	**0.03477**	**0.02454**
Order of matrix A^TA	6×6	9×9	15×15	21×21

Table 2: Parametric Table (Polynomial Estimation)

$$[C_P]_{M\times 1}=[C_{p1},C_{p2},C_{p3}.....C_{pm}] \qquad (9)$$

The objective of the least square error is to minimize the term $[\varepsilon]^T[\varepsilon]$

Where $$[\varepsilon]^T[\varepsilon] = ([C_P] - [A][\zeta])^T\ ([C_P] - [A][\zeta]) \quad (10)$$

The above minimization shall lead to the following solution for the coefficients

$$[\zeta] = (A^T A)^{-1} A^T [C_P] \quad (11)$$

For example the 4th order expression of multivariate polynomial estimation shall be as follows

$$\hat{C}_P(\lambda, \beta) = \xi_{00} + \xi_{10}\lambda + \xi_{01}\beta + \xi_{20}\lambda^2 + \xi_{11}\lambda\beta + \xi_{02}\beta^2 + \xi_{30}\lambda^3 + \xi_{21}\lambda^2\beta + \xi_{12}\lambda\beta^2 + \xi_{03}\beta^3 + \xi_{40}\lambda^4 + \xi_{31}\lambda^3\beta + \xi_{22}\lambda^2\beta^2 + \xi_{13}\lambda\beta^3 + \xi_{04}\beta^4 \quad (12)$$

It can be observed from Table 3.2 that the use of higher-order models results in improved root mean square error (RMSE), with the most significant improvement occurring when transitioning from the 3rd to the 4th order model. However, as the order of the model increases, there is a substantial increase in the size of matrix $A^T A$, leading to excessive computational load during matrix inversion. Furthermore, the improvement in RMSE diminishes with higher-order models. Therefore, the 4th order model can be selected as a compromise between estimation accuracy and computational complexity.

The RMSE (Root Mean Square Error) is the measure of the goodness of fit and can be calculated as follows

$$RMSE = \sqrt{\frac{\sum_{k=1}^{M}\left(\hat{C}_P - C\right)^2}{M}} \quad (13)$$

4. RATED AND SUB-RATED REGIME

Once we get the generic expression for power extraction coefficient C_P in terms of tip-speed ratio and the pitch angle, the power extracted by the wind turbine can be expressed by Equation (3).

If pitch angle be fixed to a certain value, the above equation expresses the values of extracted turbine power in terms of two variables namely the wind speed and the turbine speed. For different values of wind speeds, there exists a unique curve representing the variation of the turbine power with respect to the turbine rotational speed. Infinite number of such curves can be drawn for infinite number of possible wind speeds, but for simplicity only a few curves have been drawn corresponding to a few different values of the wind speeds.

By putting the values of these c-coefficients into equations (2a) & (2b), the optimal values of λ (i.e. λ_{opt}) and β (i.e. β_{opt}) can be easily found by following the procedure prescribed by equations-14 & 15. At these values, the power extraction coefficient (C_P) will be maximum.

$$\left(\frac{\partial C_P(\lambda_i, \beta)}{\partial \lambda}\right) = 0 \Rightarrow \left(\frac{\partial C_P(\lambda_i, \beta)}{\partial \lambda_i}\right)\cdot\left(\frac{\partial \lambda_i}{\partial \lambda}\right) = 0 \Rightarrow f_1(\lambda, \beta) = 0 \quad (14)$$

$$\left(\frac{\partial C_P(\lambda_i, \beta)}{\partial \beta}\right) = 0 \Rightarrow \left(\frac{\partial C_P(\lambda_i, \beta)}{\partial \lambda_i}\right)\cdot\left(\frac{\partial \lambda_i}{\partial \beta}\right) = 0 \Rightarrow f_2(\lambda, \beta) = 0 \quad (15)$$

4.1 SUB-RATED ZONE

In the region between the cut-in wind speed and the rated wind speed, known as the sub-rated region, the control objective is to maximize turbine power extraction by achieving the optimal power coefficient, C_P. In this region, the pitch angle should be maintained at its optimal value, and any variation in wind speed must be accompanied by an appropriate adjustment in the turbine's rotational speed to ensure that the tip-speed ratio remains optimal, thereby maximizing C_P. This desired turbine speed control can be achieved by adjusting the instantaneous electromagnetic torque of the generator to follow the "optimal locus" on the torque-speed curve. Other methods, such as Tip-Speed Ratio (TSR) control or Power Signal Feedback (PSF) control, are also available for managing turbine speed. However, due to the advantages that will be discussed later, this study focuses on torque-based control.

The optimal value of the extracted power in the sub-rated region can be obtained as given followed

$$(P_{WT})_{opt} = -\frac{1}{2}\rho.\pi R^2\left(\frac{\omega_T R}{\lambda_{opt}}\right)^3.C_P(\lambda_{opt},\beta_{opt}) = -\frac{\rho\pi R^5}{2}\frac{C_P(\lambda_{opt},\beta_{opt})}{\lambda^3{}_{opt}}.(\omega_T)^3 = -k_{opt}\omega_T{}^3 \qquad (16)$$

Where $$k_{opt} = \frac{\rho\pi R^5 C_P(\lambda_{opt},\beta_{opt})}{2\lambda^3{}_{opt}} \qquad (17)$$

All the operating points satisfying the above equation on the power-speed graph shall be termed as optimal operating points. The locus of the optimal operating points can be seen to be passing through the power maxima of the power-speed curves drawn for the different wind speeds (Figure 2 & 3).

At steady state optimal operating points, the turbine output torque at a given turbine speed " ω_T " shall be given by

$$(T_{WT})_{opt} = \frac{(P_{WT})_{opt}}{\omega_T} = -k_{opt}\omega_T{}^2 \qquad (18)$$

Putting it in other way, it can be said that if the instantaneous electromagnetic torque posed by the generator is made to follow the relationship $T_e = (T_{WT})_{opt} = -k_{opt}\omega_T{}^2$, the machine will reliably reach to a new optimal operating-point after following transient acceleration/deceleration because the steady-state shall prevail eventually under which T_{WT} is destined to be equal to T_e. For generating the above electromagnetic torque command, the output of the turbine-speed sensor is required on instantaneous basis. It is observed that at the different potential optimal operating points (i.e. the points of intersection of the electromagnetic torque curve w.r.t. the different turbine torque curves), the condition $\partial T_e / \partial\omega_T > \partial T_{WT} / \partial\omega_T$ is invariably achieved, which is the condition of stable operating points for generating operation. Therefore it can be concluded that all these points (p1, p2, p3 p4 etc.) shall be stable operating points (Figure 2 & 3).

Let us consider a WECS operating stably at an optimal operating point "p_1" and the current wind speed is "v_1", if wind speed increases to a new value "v_2" the turbine torque-speed characteristics will be switched from curve-1 to curve-2 and the rotor will be accelerated as dictated by the vertical-gap between the new turbine torque (curve-2) and the electromagnetic torque-speed characteristics (Figure 2 & 3). The turbine speed shall eventually settle to the new optimal operating point p_2.

Therefore the bottom line of the sub-rated region control is that if the instantaneous electromagnetic torque command is generated according to the following equation by taking the feedback from rotor-speed sensor, the steady state MPPT is always ensured.

$$T_e^* = -k_{opt}\omega_T{}^2 \qquad (19)$$

For DFIG based WECS the above command can be implemented by SFOC whereas for SCIG based system it is, in general, implemented by RFOC. The effectiveness of the above method depends on the reliability of the rotor-speed measurement sensor and on the accuracy with which the coefficient k_{opt} could be estimated. The benefit of using FOC is the fact that the electromagnetic torque control loop can be made fast enough so that the actual electromagnetic torque follows its command almost immediately.

The above torque based control has the advantages like simplicity, fast response and efficiency. But the efficiency is less in comparison to the TSR control as the wind speed is not directly measured therefore for high inertia system the change in wind speed is not quickly reflected into generator output.

4.2 RATED ZONE

It is obvious from equation-3.16 that if the tip-speed ratio and the pitch angle be maintained at λ_{opt} and β_{opt} respectively, in the course of gradually increasing wind speed, there comes a situation when the power output of the turbine shall tend to exceed beyond the rating of the generator powered by it.

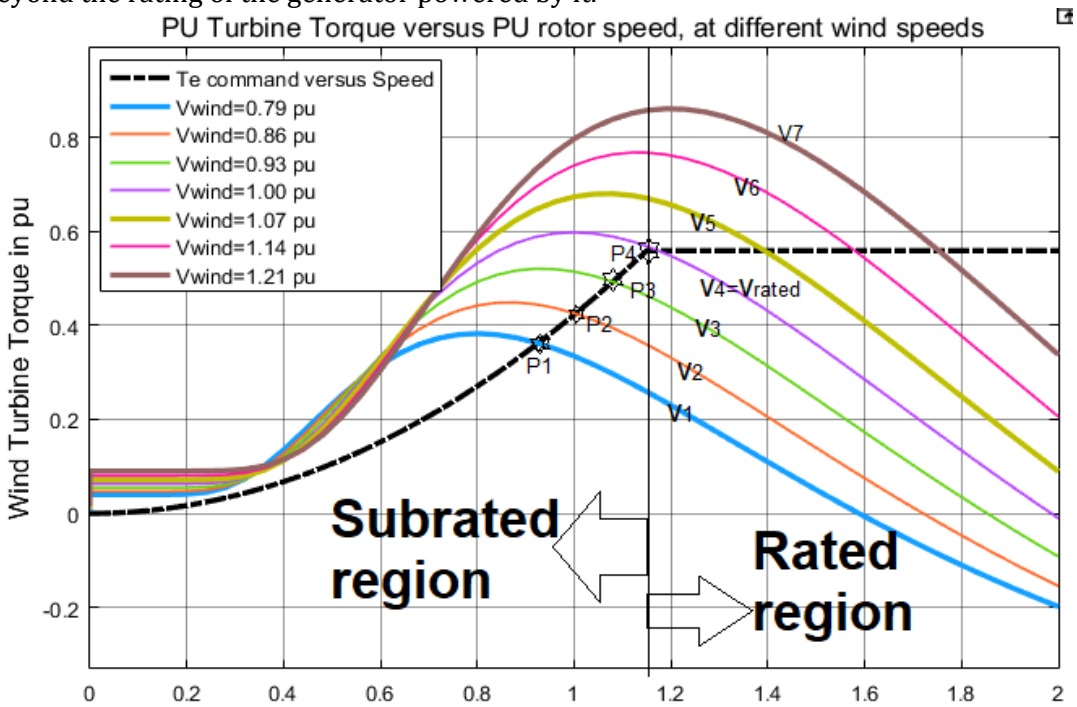

Figure 2. (Torque speed characteristics for constant torque scheme with beta=0)

This happens when the wind speed reaches its rated value. Therefore any further potential increment in the turbine power output, due to the wind speed exceeding beyond rated value, must be curtailed down so that it can be maintained at the level of the generator rating.

The rated zone commences as soon as the optimized extracted power in the sub-rated region tends to breach the rating of the generator. With the commencement of rated regime, the control objective is no more about maximizing the power extracted, but to limit & maintain it at rated value. It is obvious that in the case of wind speed going beyond rated value, maintaining the extracted power at its rated value necessitates degradation in the extraction coefficient C_P. For this to happen the restriction imposed on the variables λ and β needs to be relaxed whose values in otherwise sub-rated region were strictly maintained at optima.

This power curtailment exercise can be carried out by simultaneously controlling the electromagnetic torque command as well as the pitch-angle command.

5. EXISTING CONSTANT TORQUE-SPEED CONTROL IN THE RATED ZONE

The most commonly used strategy reported in the previous literatures are, in general, the two-fold control approach in which the generator is given a constant electromagnetic command whereas the speed of the generator is maintained at a constant rated value by generating an appropriate pitch-control command.

The graph in Figure-2 has been drawn for zero pitch angles (optimal value). It can be observed that if the system is operating at point p_4,and the pitch angle is left unperturbed at its optimal value, as soon as the speed changes to v_5 ($>v_{rated}$), the mechanical torque produced by the generator becomes greater than the electromagnetic torque. Thus the rotor accelerates and tends to settle down to the new operating point at the intersection of the electromagnetic torque curve and the new mechanical torque curve. Given that the electromagnetic torque command has been kept at a constant value, this increase in the rotor speed is unacceptable as it will result into increase in the mechanical power fed into the generator thus violating its rating. Therefore as soon as the rated wind speed is violated, the pitch-angle control must act fast enough to change the pitch angle, much before any appreciable change in the rotor speed, so that the new torque profile of the turbine could be lowered down (by changing the pitch angle) in such a way that it eventually intersects the electromagnetic torque curve again at the point p4. For any change in the wind speed beyond rated value, the pitch-

control is carried out up to the point of time until the final steady state operating point converges down to the rated operating point p_4. Although the final operating points invariably converges down to the rated operating point p_4 leading to rated power operation at final steady state, in transient duration the power fed to the generator exceeds beyond the rated value. Therefore the pitch control mechanism must be fast enough so that this transient time span is narrowed down and thus any appreciable potential increase in the rotor speed and the consequent prolonged violation of the generator rating could be obviated beforehand.

Given the procedural emergency mentioned in carrying out the above control, the obligation on the pitch-control mechanism in terms of fastness and reliability can be well appreciated.

6. PROPOSED INVERSE TOQUE-SPEED CONTROL IN THE RATED ZONE

The major disadvantage to this method can be attributed to the extreme burden on the pitch-control mechanism. This problem can be obviated by adopting the proposed inverse torque control in the rated zone.

As already mentioned that the control objective in the rated regime is to maintain the power extraction at its rated value, one of the possible alternatives could be to implement the inverse torque-speed control. In it the electromagnetic torque command is generated as per the following equation

$$T_e^* = -\frac{k_{opt}.(\omega_{T\,rated})^2}{\omega_T} = -\frac{P_{rated}}{\omega_T} \qquad (20)$$

The information about ω_T is obtained from the rotor-speed sensor.

7. RESULT & DISCUSSION

As it is assumed that in FOC environment the actual electromagnetic torque follows its command almost immediately, therefore the actual electromagnetic torque Te shall follow the relationship imposed by the Equation 20. If the pitch angle is left unperturbed at its optimal value and the system is initially operating at point p_4, as soon as the speed changes to v_5 (>v_{rated}), the mechanical torque produced by the generator becomes greater than the electromagnetic torque.

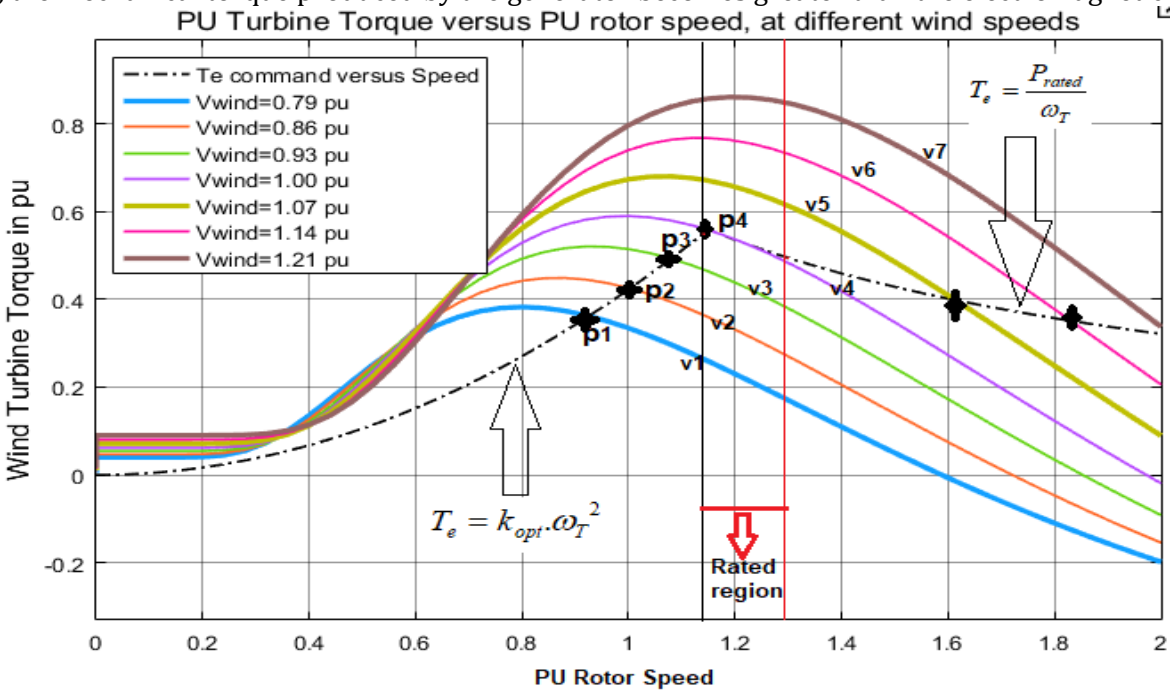

Figure 3. ((Torque speed characteristics for inverse torque scheme with beta=0)

As it is assumed that in FOC environment the actual electromagnetic torque follows its command almost immediately, therefore the actual electromagnetic torque Te shall follow the relationship imposed by the Equation (20). If the pitch angle is left unperturbed at its optimal value and the system is initially operating at point p_4, as soon as the speed changes to v_5 (>v_{rated}), the mechanical torque produced by the generator becomes greater than the electromagnetic torque. Thus the rotor accelerates and tends to settle down to the new operating point at the intersection of the electromagnetic torque curve and the new mechanical torque curve. It is obvious from the diagram that if the pitch-control mechanism

is not called upon, the rotor speed shall increase to a very high value in comparison to the previously described method. Therefore even in this case, the pitch-control mechanism (of a relatively moderate speed) must be called upon so that the new torque profile of the turbine could be lowered down in such a way that the final steady state turbine speed lies well within 130 % of the rated value.

The "Inverse Torque-speed" control block in the rated regime is as follows (Figure 3)
The superiority of this method lies in the fact that the electromagnetic power fed to the generator always remains constant even during transient acceleration/deceleration. Therefore it can be stated that the inverse torque-speed control in sub-rated regime strategy may lead to a considerable reduction in the cost of pitch control mechanism. It also relieves the stress on the pitch control mechanism.
The simulation results based on the 1D0S model have been found to be considerably different from the experimental findings whereas these differences are less for a 2D1S model. In [16], it has been demonstrated that the 1D0S model could be over-optimistic in short term voltage stability studies as it under predicts the reactive power requirement and therefore over predicts the voltage restoration time. It has been shown in [17]that the 1D0S model over estimates the fault clearing time. The result analysis has been done by taking the system parameters case from [18].

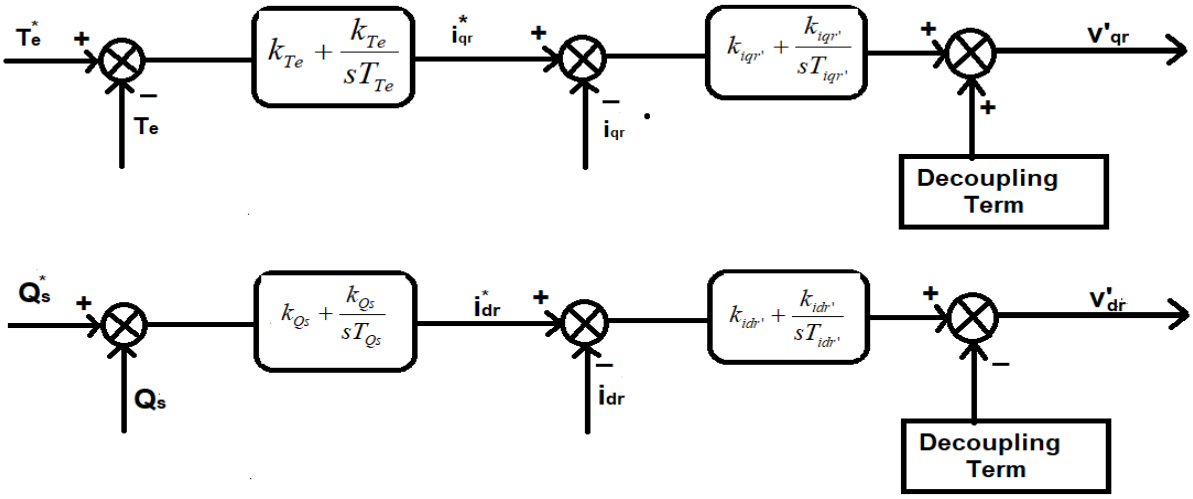

Figure 4 (Decoupled control of electromagnetic torque and the stator reactive power)

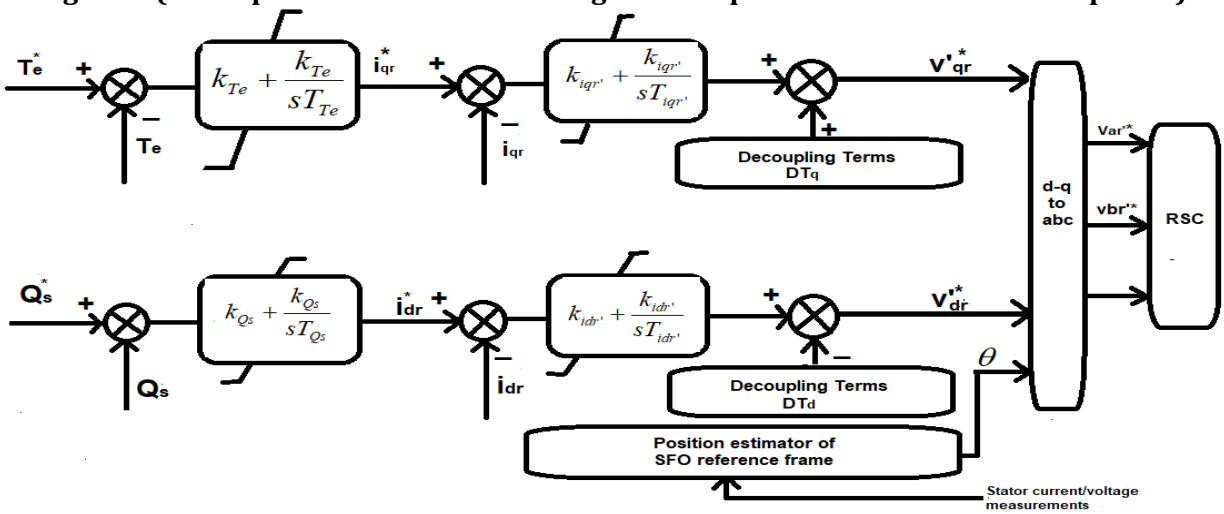

Figure 5 (Decoupled control of electromagnetic torque and the stator reactive power)

As of now the GSC has been modelled just as a current source (when viewed from the grid side). It is assumed that the current command given to GSC is such that it ensures a constant DC-link voltage and a desired level of Q_{GSC}. Usually Q_{GSC} is set to zero for getting benefits of reducing the convertor ratingFigure 4 & 5.
The decoupled MPPT control and reactive power control of a DFIG has been given in the following Figure 6 & 7.

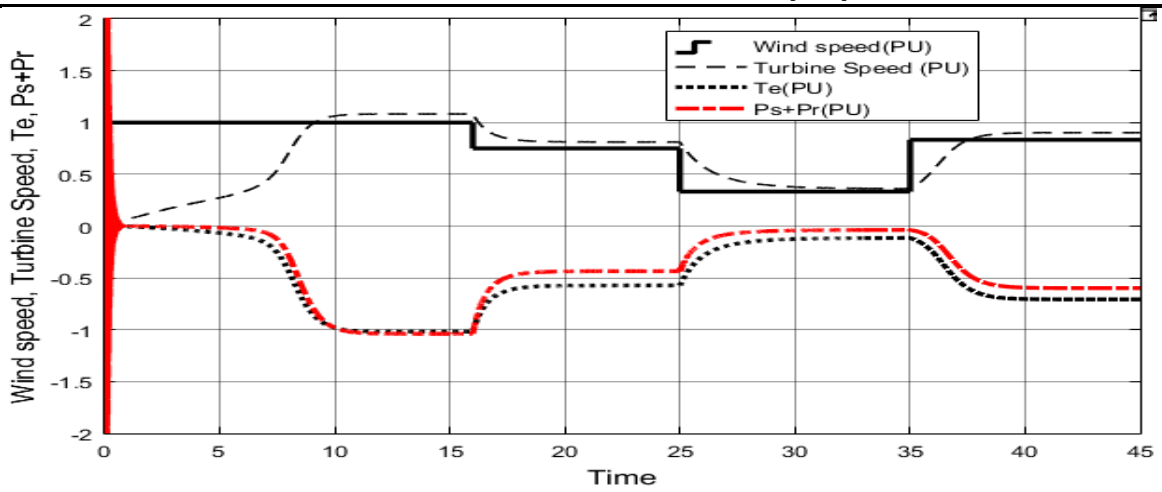

Figure 6: MPPT Control

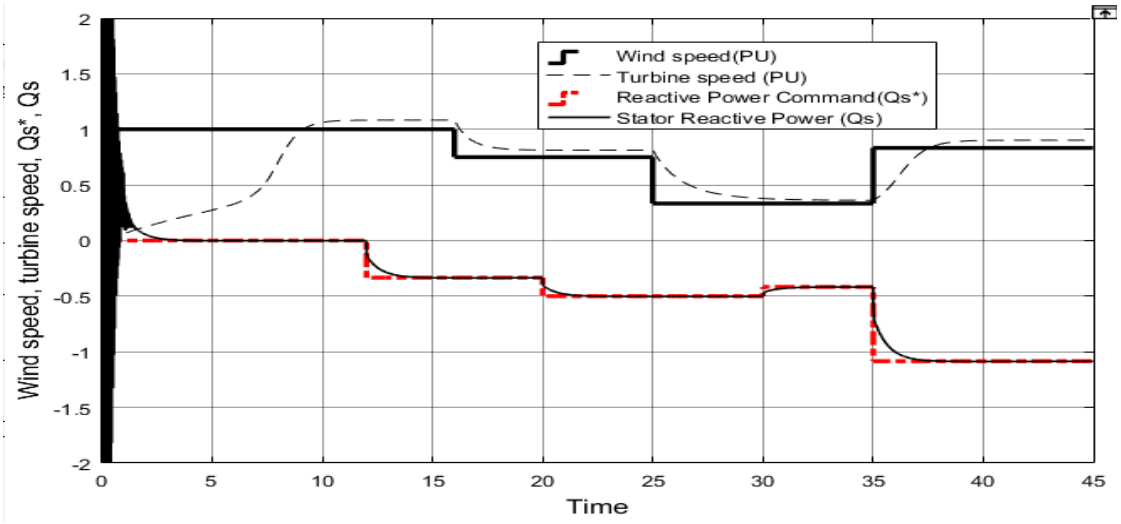

Figure 7 Reactive Power Control

CONFLICT OF INTERESTS

None.

ACKNOWLEDGMENTS

None.

REFERENCE

Coyle, Eugene D. and Simmons, Richard A., Understanding the Global Energy Crisis (2014). Purdue University Press. (Knowledge Unlatched Open Access Edition.)

Guozhu Mao, Xi Liu, Huibin Du, Jian Zuo, Linyuan Wang, Way forward for alternative energy research: A bibliometric analysis during 1994â€“2013,Renewable and Sustainable Energy Reviews, Volume 48, 2015, Pages 276-286,ISSN 1364-0321, https://doi.org/10.1016/j.rser.2015.03.094.

Morris, Philip & Long, Lyle &Brentner, Kenneth. (2004). AnAeroacoustic Analysis of Wind Turbines. Collection of ASME Wind Energy Symposium Technical Papers AIAA Aerospace Sciences Meeting and Exhibit. 10.2514/6.2004-1184.

Tongguang Wang, A brief review on wind turbine aerodynamics, Theoretical and Applied Mechanics Letters, Volume 2, Issue 6, 2012, 062001, ISSN 2095-0349

Capuzzi, Marco &Pirrera, Alberto & Weaver, Paul. (2015). Structural design of a novel aeroelastically tailored wind turbine blade. Thin-Walled Structures. 95. 7-15. 10.1016/j.tws.2015.06.006.

T. Petru and T. Thiringer, “Modeling of wind turbines for power system studies,”IEEE Trans. Power Syst., vol. 17, no. 4, pp. 1132–1139, Nov. 2012.

Branlard, Emmanuel. (2017). The blade element momentum (BEM) method. 10.1007/978-3-319-55164-7_10.

Sheng, W..(2019). A revisit of Navier-Stokes equation.

Algazin, Sergey. (2007). Numerical study of Navier-Stokes equations.Journal of Applied Mechanics and Technical Physics. 48. 656-663. 10.1007/s10808-007-0084-x.

Hansen, M. O. L., and Aagaard Madsen, H. (October 19, 2011). "Review Paper on Wind Turbine Aerodynamics."ASME. J. Fluids Eng. November 2011; 133(11): 114001.

H. Snel, “Review of aerodynamics for wind turbines,” Wind Energy, vol. 6, no. 3,pp. 203–211, June 2003.

PoulSÃ¸rensen, Anca D. Hansen, Pedro AndrÃ© Carvalho Rosas, Wind models for simulation of power fluctuations from wind farms, Journal of Wind Engineering and Industrial Aerodynamics, Volume 90, Pages 1381-1402, ISSN 0167-6105.

T. Petru and T. Thiringer, “Modeling of wind turbines for power system studies,” IEEE Trans. Power Syst., vol. 17, no. 4, pp. 1132–1139, Nov. 2002.

G. Son, H. L. Lee and J. Park, "Estimation of Wind Turbine Rotor Power Coefficient Using RMP Model," 2009 IEEE Industry Applications Society Annual Meeting, 2009, pp. 1-8, doi: 10.1109/IAS.2009.5324837.

González-Hernández, J. G., & Salas-Cabrera, R. (2019). Representation and estimation of the power coefficient in wind energy conversion systems.RevistaFacultad De Ingeniería, 28(50), 77–90. https://doi.org/10.19053/01211129.v28.n50.2019.8816.

Guided Tour on Wind Energy, http://ele.aut.ac.ir/~wind/en/tour/index.htm

S. K. Salman, A. L. J. Teo, and I. M. Rida, “The effect of shaft modelling on the assessment of fault CCT and the power quality of a wind farm,” in Proc. of Harmonics and Quality of Power Int. Conf., vol. 3, Oct. 2000, pp. 994–998.

Choudhary, R., Jyotiraditya, K., & Mahto, D. (2024). Simplified modelling of induction generator in stator flux oriented synchronous reference frame. *Shodhkosh: journal of visual and performing arts*, *5*(7), 16–26. Https://doi.org/10.29121/shodhkosh.v5.i7.2024.1774.